Lab on a Chip

PAPER

View Article Online
View Journal | View Issue

Published on 14 February 2017. Downloaded by UNIVERSITY OF CINCINNATI on 15/03/2017 12:06:03.

Cite this: *Lab Chip*, 2017, **17**, 1069

Electrowetting without external voltage using paint-on electrodes†

Collin B. Eaker,[a] Ishan D. Joshipura,[a] Logan R. Maxwell,[a] Jason Heikenfeld[b] and Michael D. Dickey*[a]

Electrowetting uses voltage to manipulate small volumes of fluid for applications including lab-on-a-chip and optical devices. To avoid electrochemical reactions, a dielectric often separates the fluid from the electrode, which has the undesired effect of adding processing steps while increasing the voltage necessary for electrowetting. We present a new method to dramatically reduce the complexity of electrode and dielectric fabrication while enabling multiple performance advances. This method relies on a self-oxidizing paint-on liquid-metal electrode that can be fabricated in minutes on rigid, rough, or even elastic substrates, enabling low operation voltages (<1 V), and self-healing upon dielectric breakdown. Furthermore, due to the non-negligible 'potential of zero charge', electrowetting occurs by simply short circuiting the electrodes. This work opens up new application spaces for electrowetting (*e.g.* stretchable substrates, soft and injectable electrodes) while achieving large changes in contact angle without the need for an external power supply.

Received 6th December 2016,
Accepted 14th February 2017

DOI: 10.1039/c6lc01500j

rsc.li/loc

Reprinted from Lab on a Chip

Introduction

Electrowetting is a technique used to manipulate liquid drops on a substrate.[1,2] It is useful for microfluidic applications including liquid lenses,[3] displays,[4,5] and miniature bioassays.[6,7] Unlike electrocapillarity,[8] electrowetting is driven by an electromechanical force and does not involve a change in interfacial tension. Applying a potential to the fluid of interest (often water) relative to an electrically insulated counter electrode generates the required electrical charge. The electrical insulation (dielectric) prevents Faradaic electrochemical reactions from occurring in the liquid (*e.g.*, electrolysis of water). This configuration is called electrowetting-on-dielectric (EWOD) and is the most common electrowetting technique for actuating fluids. As applied voltage is increased, the liquid changes its apparent contact angle to lower its capacitive energy. An ideal EWOD system should achieve maximum changes in contact angle with minimal applied voltage.

However, fabricating an ideal electrode for EWOD is typically a challenging process, especially when low voltage operation (<15 V) is desired. The dielectric coated atop a conductive metal film or doped Si wafer[9] is often achieved *via* thermal oxidation, sputtering, thermal evaporation, or atomic layer deposition. An ideal dielectric exhibits a large electrical capacitance and is free of pin holes to prevent electrical shorts through the insulator. Electrowetting dielectrics are commonly hundreds of nanometers to several microns thick to ensure sufficient insulation between the liquid and the electrode.[10] However, thicker dielectrics necessitate larger voltages. Furthermore, reducing the dielectric thickness is often insufficient, because the required voltage decreases only as the square root of the thickness.[11] Some clever resolutions have been developed to mitigate dielectric breakdown, including multilayers of dielectrics,[11] self-healing dielectrics,[12] and utilization of two immiscible electrolytes.[13]

Here, we demonstrate a unique approach for creating self-healing, low-voltage, battery-free, and even stretchable electrowetting systems. In this work, an electrode composed of eutectic gallium indium (EGaIn, 75% Ga, 25% In by weight)[14] or pure gallium can be simply painted on a substrate (*e.g.* glass) at room temperature. Due to the low melting point (~15.5 °C) of EGaIn, the metal is liquid at room temperature and forms a thin (~1–3 nm)[15,16] passivating oxide layer. This oxide forms spontaneously in the presence of oxygen and serves to mechanically stabilize the liquid metal in the shape of a film. This work takes advantage of the thin, self-forming oxide as a dielectric for electrowetting.

Using an EGaIn electrode is a simple approach that solves numerous electrowetting challenges: (i) unlike traditional EWOD dielectrics, EGaIn can be applied to a surface quickly, at room temperature, and without vacuum processing. This

[a] *Department of Chemical and Biomolecular Engineering, North Carolina State University, Raleigh, NC 27695-7905, USA. E-mail: mddickey@ncsu.edu*
[b] *Department of Electrical Engineering and Computing Systems, University of Cincinnati, Cincinnati, OH 45221-0030, USA*

† Electronic supplementary information (ESI) available. See DOI: 10.1039/c6lc01500j

Published on 14 February 2017. Downloaded by UNIVERSITY OF CINCINNATI on 15/03/2017 12:06:03.

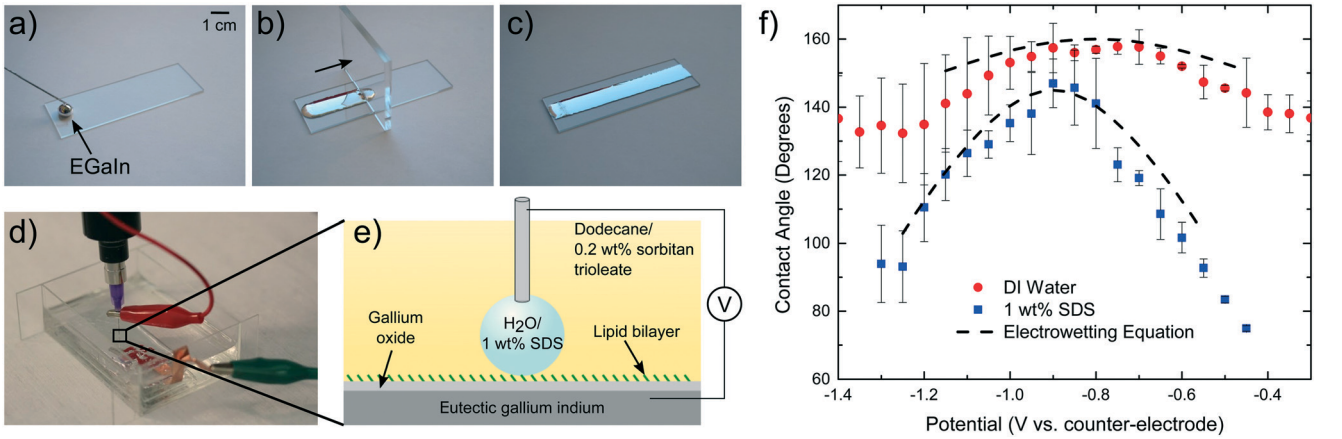


Fig. 1 Preparation of the 'paint on' liquid metal electrodes for low-voltage electrowetting. (a–c) 100 μL drop of EGaIn is placed on a glass substrate and spread as a film across the surface. (d and e) A DI H_2O/1 wt% SDS drop is submerged in dodecane/0.2 wt% sorbitan trioleate solution and voltage is applied across a top electrode (a stainless steel dispensing needle) and the EGaIn layer. (f) DC electrowetting curve of DI H_2O and H_2O/1 wt% SDS, including theoretical curves. Error bars represent s.d.

process is shown in Fig. 1. (ii) As a liquid, EGaIn conforms to both non-planar and stretchable substrates. (iii) The Ga oxide on EGaIn can support self-assembled lipid bilayers[17,18] that enable large contact angle changes (>100°) for water by applying small voltages (100s of mV). (iv) The anodic nature of the oxide and the self-assembly of the lipid bilayer allows the dielectric layer to self-heal upon breakdown.[12] (v) Perhaps most interestingly, the small voltages required to induce changes in contact angle in this system reveal the effects of the so-called 'potential of zero charge', which allows significant electrowetting to occur simply by shorting the electrodes without the need for an external voltage.

The potential of zero charge, V_{PZC}, is the electric potential at which the plot of apparent contact angle *versus* potential (*i.e.* the electrowetting curve) reaches a maximum. It can be understood by considering the Lippmann–Young equation,[1] which models the contact angle change in response to voltage across an electrowetting interface as shown in eqn (1),

$$\cos\theta(V) = \cos\theta_Y + \frac{C(V - V_{PZC})}{2\gamma_{wo}} \quad (1)$$

where θ is the contact angle of the liquid as a function of applied voltage (V), θ_Y is the Young's angle (*i.e.*, the angle in the absence of applied voltage), C is the capacitance of the dielectric normalized by area in contact with the liquid, V is the applied voltage, V_{PZC} is the potential of zero charge, and γ_{wo} is the interfacial tension between the two liquids (*e.g.* water and oil). The V_{PZC} is a function of surface potential, electrolyte composition, and the composition of the top and bottom electrodes. According to eqn (1), the V_{PZC} causes the electrowetting curve to be centered away from zero volts.[19] In most electrowetting systems, however, inducing changes in contact angle requires application of tens[20] to hundreds[21] of volts. These voltages are significantly larger than the V_{PZC} (<1 V); therefore, the electrowetting curve often appears to center at zero volts. Thus, in practice, the V_{PZC} is neither experimentally significant nor discernable.

In the system described here, the voltages needed to induce electrowetting are extremely low (similar in magnitude to the V_{PZC}) due to the very large capacitance (arising from the thin dielectric) and the low γ_{wo} (arising from the use of surfactants). Furthermore, the materials of construction render a large V_{PZC}. Consequently, significant electrowetting occurs by simply short-circuiting the electrodes without an external potential present. Stated differently, eqn (1) evaluated at $V = 0$ results in a significant change in contact angle since V_{PZC} is non-negligible. Consequently (and in contrast to conventional EWOD), increasing the potential relative to 0 V increases the contact angle of the liquid droplet; thus, it is possible to electro-dewet a droplet under these circumstances.

In this paper, we outline the fabrication of these EGaIn electrodes, characterize their electrowetting behavior, describe the wetting of drops of water when short-circuited with the electrode, and demonstrate the robustness of the electrowetting while stretching of the underlying substrate. These unconventional materials are compatible with microfluidic systems, in the form of injectable electrodes,[22,23] potentially leading to new applications.

Methods and materials

Substrate fabrication

We fabricated the electrodes by first constructing a spreader tool (similar to a slot die with a gap of 50 μm) out of polymethylmethacrylate (PMMA) using a laser cutter. Dragging the spreader along the length of the 1 × 3″ glass slide established a thin and shiny film from a 100 μL drop of EGaIn. The film was spread across a piece of copper tape on the substrate, to form an electrical connection. This method was also used for the gallium electrode, with the gallium placed in a freezer until it solidified. For the rough film, a 20 μL drop was brushed across the glass surface with a cloth

Reprinted from Lab on a Chip

 This journal is © The Royal Society of Chemistry 2017

Published on 14 February 2017. Downloaded by UNIVERSITY OF CINCINNATI on 15/03/2017 12:06:03.

until a continuous film was established across the entire surface.

DC electrowetting

The contact angle of the water drop was recorded at equilibrium upon applying a DC voltage. A contact angle goniometer (manufactured by First Ten Angstroms) recorded the contact angle of the droplet simultaneously. De-ionized water or a solution of water and 1 wt% sodium dodecyl sulfate were dispensed within the oil with a 30 gauge stainless steel syringe needle. Electrical experiments were performed with Agilent E3612A power source. Electrical connections were made to the copper tape on the substrate, and to the syringe needle. The positive terminal of the power source was connected to the stainless steel syringe tip. Meanwhile, the negative terminal was connected to the Cu tape. The negative terminal was also grounded to the source meter. A Fluke multimeter connected in parallel to the Agilent power source was used to verify the applied voltage. Potential was applied from −1.40 V to −0.30 V for the DI water, and −1.30 V to −0.45 V for the SDS/water, in 50 mV increments. The results shown in Fig. 2 represent the average contact angle at the respective voltage from three trials. The error bars show the standard deviation of contact angle from the three trials.

Beyond −1.1 V, the water droplet cannot achieve an equilibrium contact angle due to dielectric breakdown. In the breakdown regime, the water droplet moves spatially, which results in asymmetric contact angle between left and right side of droplet. The asymmetry of the drop is the cause for high standard deviation of contact angle beyond −1.1 V.

AC electrowetting

All AC electrowetting experiments use a two-electrode configuration. A Gamry Reference 600 potentiostat applied a −800 mV DC offset with respect to the stainless steel counter-electrode at 100 Hz (sine waveform). The experiments were performed from 0 mV RMS to 800 mV RMS, in 50 mV increments; they were also performed in both directions, to test for hysteresis. The potential was applied on for at least one minute to allow the contact angle to reach equilibrium.

Stretchable electrowetting

The stretchable substrates were prepared in the same manner as the glass slides. The EGaIn was spread across a 3 cm × 1.25 cm piece of Ecoflex. The Ecoflex was then stretched to 6 cm, and clipped down to a glass slide to hold the strain in place.

Wetting by short-circuit

The experiments were performed by directly connecting the copper tape attached to the substrate and the stainless steel syringe needle.

Variable electrodes

23 gauge polypropylene syringe tips were used to dispense DI water. The top electrode material was inserted into the plastic above the syringe tip through a hole drilled into the wall of the syringe tip (to make a connection to the water), and connected to the potentiostat. EGaIn and gallium were injected into Tygon® tubing and then sealed above the tip in the same manner. Linear sweep voltammetry was performed using a Gamry Reference 600 potentiostat. The potential was then swept at 1 mV s^{-1} from −1.5 V to −0.2 V with respect to the counter-electrode for the case of platinum, stainless steel, and copper. For gallium and EGaIn, the potential was swept from −0.5 V to 0.5 V with respect to the counter-electrode, and the resulting contact angle and current were measured. This method was then repeated, with a reference electrode, along with the counter-electrode. To fabricate the reference electrode, a silver wire was inserted into Tygon tubing that was filled with an agar hydrogel. The hydrogel was made by placing 2 wt% agar into a solution of saturated silver chloride

Reprinted from Lab on a Chip

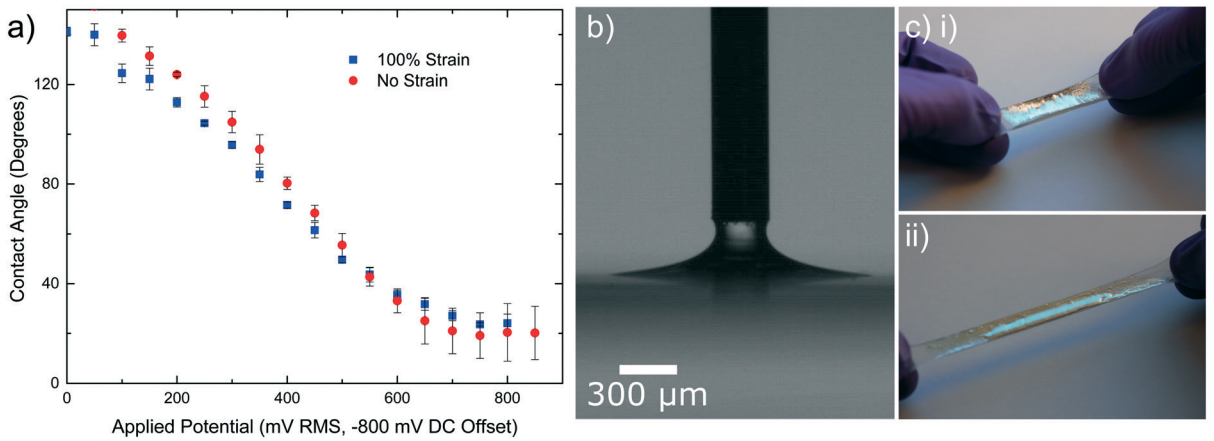


Fig. 2 Electrowetting on a stretchable substrate. (a) AC electrowetting curve on EGaIn, with both no strain and 100% strain of the underlying substrate. (b) Minimum reversible contact angle achieved (7°) with AC electrowetting at −800 mV RMS applied. (c) Photographs of i) EGaIn film on a substrate made of silicone elastomer. ii) Liquid metal conforms to the elastomer and elongates when the substrate is stretched.

Published on 14 February 2017. Downloaded by UNIVERSITY OF CINCINNATI on 15/03/2017 12:06:03.

in 3.5 M potassium chloride, heating the solution, and then injecting into the tubing. Once the reference and counter-electrode were inserted, a linear sweep was performed at 1 mV s^{-1} for each metal, from −1.5 V to −0.2 V with respect to the Ag/AgCl reference. From this, the contact angle and current were simultaneously measured.

Results

We fabricate the electrodes by dragging a 100 μL droplet of EGaIn along the length of a glass slide using a custom-built slot die coater. This process establishes a thin and shiny film of EGaIn, as seen in Fig. 1a–c. A strip of copper tape under the liquid metal forms an electrical connection. The entire apparatus rests on the stage of a contact angle goniometer (Fig. 1d).

The liquid metal electrode supports a droplet of deionized water (DI H_2O) with 1 wt% sodium dodecyl sulfate (SDS). A stainless-steel electrode connects to the top of the water droplet, as shown in Fig. 1e. The entire system is submerged in a solution of dodecane containing 0.2 wt% sorbitan trioleate (a non-ionic surfactant). Surfactants are typically used in electrowetting to lower the energetic penalty associated with increasing meniscus surface area (spreading, wetting) and therefore increase the responsiveness of the liquid to voltage. Previous studies show that sorbitan trioleate forms a lipid bilayer between the drop of water and substrate,[17] which is evidenced here by the lack of wetting between the liquid and substrate. In this case, the lipid bilayer lowers the interfacial surface tension of the SDS/water solution to a very low level of ~0.2 mN m^{-1}, based on pendant drop analysis. Due to the thin dielectric utilized in this system, small voltages were utilized to avoid dielectric breakdown; this low interfacial tension allows large contact angle changes to occur at these voltages.

The experimental configuration in Fig. 1 is representative of a typical EWOD system. Here, the dielectric is the gallium oxide that forms spontaneously on the surface of the liquid metal along with the lipid bilayer that self-assembles on the oxide (with a total thickness of approximately 3–5 nm, ESI†). The native oxide on the liquid metal is hydrophilic (DI water contact angles ~5–10 degrees). It is possible to add a hydrophobic coating (*e.g.* Fluoropel) to the oxide surface to allow its use in air, but that coating decreases the capacitance and electrowetting requires larger voltages. The oil/surfactant mixture in this system is therefore important because it renders the oxide surface hydrophobic and decreases the interfacial tension of the water. Fig. 1f shows the electrowetting curve for an applied DC potential. These curves show dramatic contact angle changes (70–80° changes over 400 mV for a solution of DI H_2O/1 wt% SDS), with the parabolic shapes indicating classic electrowetting behavior. Importantly, the curve reaches a maximum away from zero volts (approximately −900 mV) for both fluids. This maximum of contact angle identifies the potential of zero charge (V_{PZC}). The largest changes in contact angle occurs at −1.3 V and −0.5 V, which are approximately 0.4 V from the V_{PZC}. At these terminal potentials, satellite droplets emerge from the contact line of water and lipid bilayer, which has also been observed at occurrence of electrowetting saturation.[24] These values also agree well with the theoretical curves given by eqn (1), plotted using the experimentally measured capacitance (ESI†). In each case, the droplets showed full reversibility, dewetting from the substrate and beading up into a spherical shape upon removal of the potential. The wetting behavior continues to be fully switchable even after dielectric breakdown occurs. This recovery is due to the self-healing nature of the oxide layer of the liquid metal and subsequent reassembly of the lipid bilayer.

AC potentials are known to increase the stability of the contact line in electrowetting by preventing either charge trapping or degradation,[25,26] and thereby improve reproducibility and minimize dielectric breakdown. In addition to exploring the DC behavior, we also employed an AC potential with a −800 mV DC offset to account for the potential of zero charge. This offset centers the electrowetting curve about zero volts, as shown in the electrowetting curve plotted in Fig. 2a. The contact angle shows a substantial decrease (~130° change) with the application of only 700 mV RMS. Furthermore, we observe contact angle saturation[27] at an average value of 20° (Movie S1†) with a minimum observed value of 7°, as shown in Fig. 2b. The low value of saturation is desirable, as saturation occurs near 60–80° for traditional aqueous EWOD systems,[28] with lower values (15–30°)[29] being observed with ionic liquids. As expected, the AC electrowetting results show significantly less variance than the DC electrowetting, and the contact line remained stable over the duration of the tests (up to several hours), with no observed satellite droplets. In addition, sequentially increasing and decreasing the amplitude of the AC potential provided no signs of contact angle hysteresis in the system (ESI†). The lack of hysteresis with use of AC potential is consistent with results both theoretically and experimentally proven by Mugele and colleagues.[30]

The formation of the oxide layer on the liquid metal surface provides several advantages that have been utilized for this work. In addition to stabilizing the film[24,26] of liquid metal (such that it does not bead up into a sphere due to surface tension of the metal), the oxide also allows EGaIn to adhere to a variety of substrates (*e.g.* glass, silicon, polymers). Here, we utilize a stretchable, silicone-based elastomer (Ecoflex, Smooth-on, Inc.) to test electrowetting with a strained electrode. Previous work has shown electrowetting on curved and flexible[31] substrates but, to the best of our knowledge, none have shown electrowetting on a stretchable material. Most of the conductors and dielectrics used in EWOD are comprised of rigid materials that crack at small strains; in contrast, the liquid metal forms an inherently stretchable electrode. Fig. 2c shows photographs of a film of EGaIn on an elastomeric substrate. We elongated the substrate to 100% tensile strain and performed electrowetting. The liquid metal on stretched Ecoflex shows similar

Reprinted from Lab on a Chip

 This journal is © The Royal Society of Chemistry 2017

Published on 14 February 2017. Downloaded by UNIVERSITY OF CINCINNATI on 15/03/2017 12:06:03.

electrowetting behavior as liquid metal on a glass substrate. The drawback, however, was minor swelling that occurred over time in the Ecoflex due to the dodecane immersion fluid.

Until now, all the reported experiments were performed on smooth liquid metal surfaces for consistency and simplicity of analysis (note that these thicker liquid electrodes are smooth irrespective of the smoothness of the substrate). However, EWOD on gallium-based alloys does not require a pristine surface with a smooth liquid interface. Applications may instead call for thin films of the liquid metal or solid surfaces. Fig. 3a and b show a thin film of liquid EGaIn and a film of solidified gallium, respectively. The EGaIn was prepared by brushing a 20 μL drop across the surface of a glass slide. The gallium was prepared in the same manner as demonstrated in Fig. 1 and then solidified in a freezer (m.p. ~30 °C). In spite of the surface heterogeneity present on the EGaIn film, the difference in contact angle change from the pristine EGaIn surface was negligible (albeit with more variance). Similar results were seen with solidified gallium, indicating that the electrowetting is dependent on the surface properties of the gallium oxide, rather than the phase of the underlying electrode.

Perhaps the most interesting aspect of the liquid metal electrodes is that V_{PZC} is approximately −800 to −900 mV (*vs.* the stainless steel counter-electrode); this value is also consistent with the measured open circuit potential, which generally measured in the range of −800 mV to −1.0 V. Because of the low voltages needed to induce electrowetting, the V_{PZC} must be taken into account.[19,32] As a consequence of this offset, simply closing the circuit between the EGaIn and top electrode causes significant droplet wetting by effectively bringing the system ~800 mV away from the V_{PZC} (Fig. 4, Movie S2†). This wetting is reversible; opening the circuit causes the droplet to dewet the substrate. This process may be cycled between the short circuit (wetting) and the open circuit potential (dewetting) for thousands of cycles, although leaving the system short-circuited for extended periods of time results in thickening of the oxide (ESI†). An implication

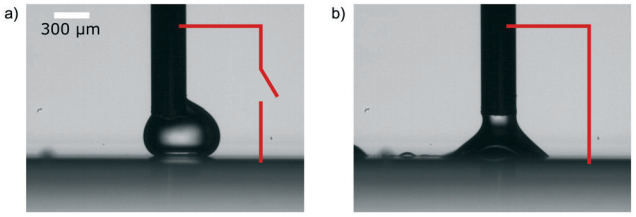


Fig. 4 Wetting of a droplet on EGaIn without externally applied potentials, with red lines representing electrical contact. (a) At open circuit, the droplet maintains a large contact angle with the substrate. (b) When the circuit is closed, the drop rapidly (and reversibly) wets the substrate due to the offset from the V_{PZC}.

of this phenomenon is that applying a potential (relative to a shorted system) causes dewetting, as evident by the electrowetting curve (*cf.* Fig. 1f).

The ability to induce wetting without an external voltage source is due to the non-negligible V_{PZC}. Previous work has shown that the V_{PZC} is a function of the surface potential, electrolyte composition, and the composition of the top and bottom electrodes.[32] Since the V_{PZC} appears to occur at the same value for DI water and SDS solutions, we instead varied the metal used in the top electrode to shift the V_{PZC}. We utilized both solid and liquid conductors for the top electrode, including stainless steel, copper, platinum, solid gallium, and EGaIn while measuring the resulting electrowetting curve (Fig. 5a) by linearly sweeping the potential at 1 mV s^{-1} using DI water. In each case, the shape of the electrowetting curve remains similar, but each one shows a distinct offset of the peak. Furthermore, a symmetric system (with either EGaIn or gallium as the top electrode) shows an apex approaching zero volts. The results here imply that simply changing the materials of construction of the top electrode is a simple way to shift the electrowetting behavior. The current profiles (Fig. 5b) align with the key features in the electrowetting curves (Fig. 5a); there is no current at the apex for each electrowetting curve, while there is current from dielectric breakdown at the potentials where contact angle begins to

Reprinted from Lab on a Chip

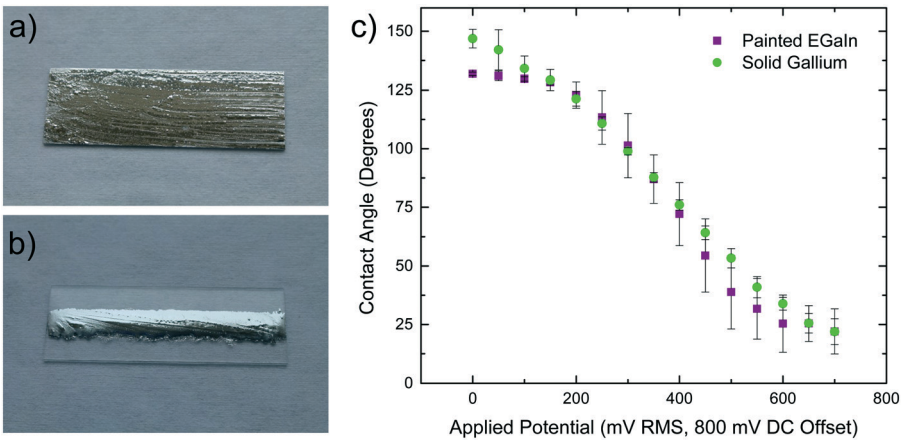


Fig. 3 Electrowetting on metal with various fabrication techniques. a) "Painted" EGaIn film that was brushed roughly across substrate. b) Solid gallium film prepared by spreading liquid Ga with a slot-die and then frozen. c) Electrowetting curve that shows similar behavior between these films and "pristine" liquid metal surface.

Published on 14 February 2017. Downloaded by UNIVERSITY OF CINCINNATI on 15/03/2017 12:06:03.

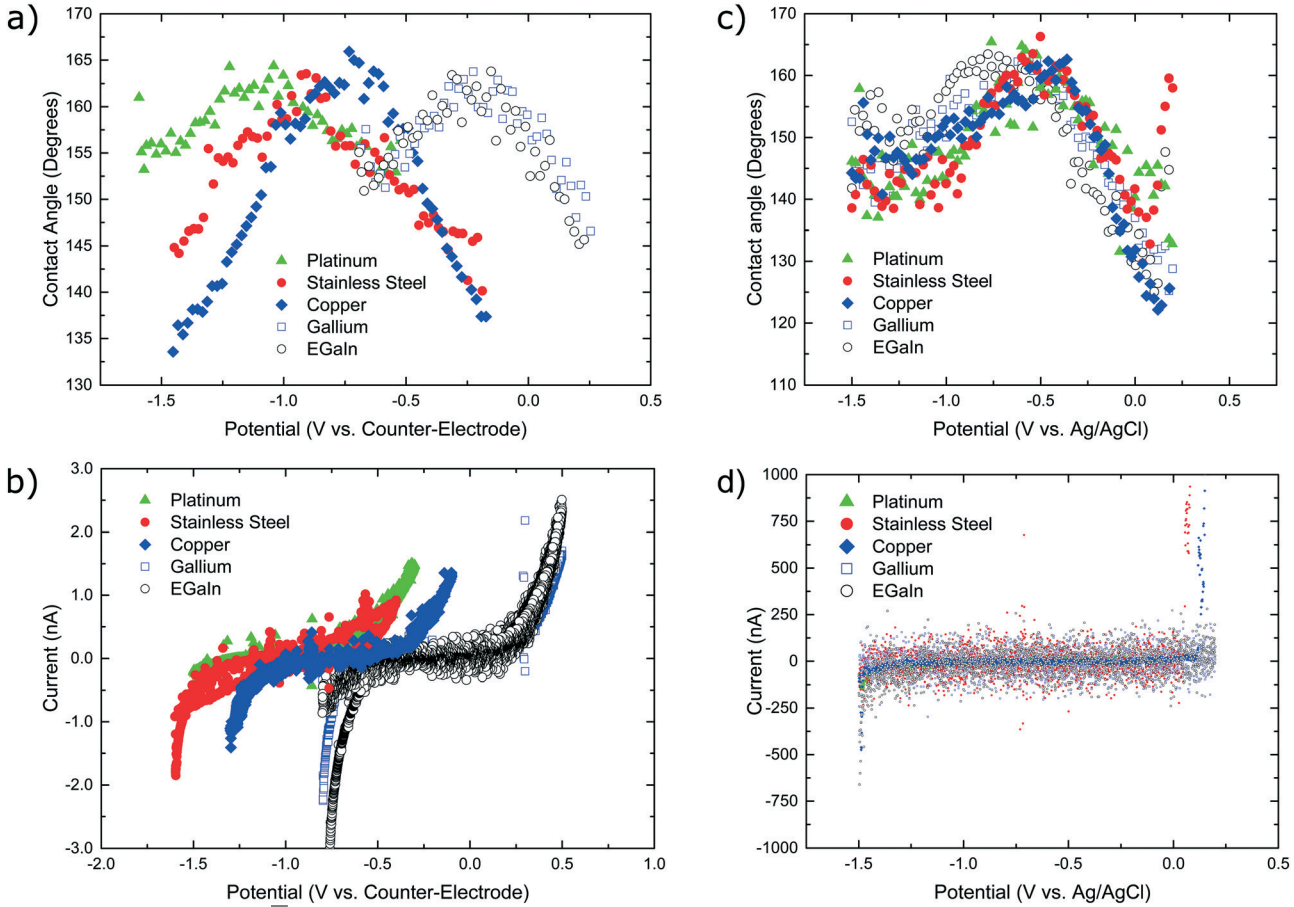


Fig. 5 The point of zero charge varies with materials of construction. (a) Electrowetting curve of DI water with platinum, stainless steel, copper, gallium, and EGaIn top electrodes. EGaIn film serves as the substrate electrode for electrowetting. (b) Linear sweep voltammogram of two-electrode system at 1 mV s^{-1}. (c) Electrowetting curve of DI water with varied top electrodes and Ag/AgCl reference electrode. (d) Linear sweep voltammogram of three-electrode system at 1 mV s^{-1}.

Lab on a Chip

saturate. Replicating the electrowetting curve with a Ag/AgCl reference electrode inserted into the solution causes the apex of the respective curves to center near a single value (approximately −0.6 V *vs.* Ag/AgCl) (Fig. 5c). This collapse occurs because the Ag/AgCl reference electrode replaces the role of the top electrode in defining the V_{PZC}. Moreover, the current profiles in Fig. 5d indicate that current only occurs away from the apex of the curves.

Conclusions

This paper demonstrates a robust system for electrowetting-on-dielectric that is simple to fabricate, self-healing, stretchable, and operates at low voltages to achieve reversible wetting and dewetting. This system is also capable of inducing wetting without an external potential due to the low interfacial tension of the droplet and the non-negligible 'potential of zero charge' arising from the materials of construction. Applying a potential relative to this shorted configuration results in dewetting, reaching a maximum contact angle at the potential of zero charge. The combined simplicity of this system and its ability to electrowet without externally applied voltage provides a simple strategy to manipulate liquid droplets. These unconventional electrodes may also enable or facilitate electrowetting in new settings, such as within microfluidics (*e.g.* injectable electrodes), across rough surfaces, and on stretchable substrates.

Author contributions

All authors contributed to experimental design. CBE, IDJ, and LRM carried out experiments. CBE and IDJ carried out data analysis. CBE, IDJ, JH, and MDD wrote the manuscript. MDD and JH supervised the research. The authors declare no competing financial interests.

Acknowledgements

MDD gratefully acknowledges support from AFRL, NSF (CMMI-0954321), and U.S. Army Research Office (ARO) (Contract No. W911NF-13-C-0045). The authors appreciate helpful conversations with Frieder Mugele, Jakub Kedzierski, Ed Bowden, and Karen Daniels.

This journal is © The Royal Society of Chemistry 2017

Published on 14 February 2017. Downloaded by UNIVERSITY OF CINCINNATI on 15/03/2017 12:06:03.

References

1 F. Mugele and J. C. Baret, Electrowetting: From basics to applications, *J. Phys.: Condens. Matter*, 2005, **17**, R705–R774.
2 R. Shamai, D. Andelman, B. Berge and R. Hayes, Water, electricity, and between… On electrowetting and its applications, *Soft Matter*, 2007, **4**, 38–45.
3 S. Kuiper and B. H. W. Hendriks, Variable-focus liquid lens for miniature cameras, *Appl. Phys. Lett.*, 2004, **85**, 1128–1130.
4 R. A. Hayes and B. J. Feenstra, Video-speed electronic paper based on electrowetting, *Nature*, 2003, **425**, 383–385.
5 B. Sun, K. Zhou, Y. Lao, J. Heikenfeld and W. Cheng, Scalable fabrication of electrowetting displays with self-assembled oil dosing, *Appl. Phys. Lett.*, 2007, **91**, 11106.
6 S. K. Cho, H. J. Moon and C. J. Kim, Creating, transporting, cutting, and merging liquid droplets by electrowetting-based actuation for digital microfluidic circuits, *J. Microelectromech. Syst.*, 2003, **12**, 70–80.
7 Y.-H. Chang, G.-B. Lee, F.-C. Huang, Y.-Y. Chen and J.-L. Lin, Integrated polymerase chain reaction chips utilizing digital microfluidics, *Biomed. Microdevices*, 2006, **8**, 215–225.
8 D. C. Grahame, The Electrical Double Layer and the Theory of Electrocapillarity, *Chem. Rev.*, 1947, **41**, 441–501.
9 S. Arscott, Electrowetting at a liquid metal-oxide-semiconductor junction, *Appl. Phys. Lett.*, 2013, **103**, 144101.
10 H. Moon, S. K. Cho, R. L. Garrell and C.-J. Kim, Low voltage electrowetting-on-dielectric, *J. Appl. Phys.*, 2002, **92**, 4080.
11 A. Schultz, S. Chevalliot, S. Kuiper and J. Heikenfeld, Detailed analysis of defect reduction in electrowetting dielectrics through a two-layer 'barrier' approach, *Thin Solid Films*, 2013, **534**, 348–355.
12 M. Dhindsa, J. Heikenfeld, W. Weekamp and S. Kuiper, Electrowetting without Electrolysis on Self-Healing Dielectrics, *Langmuir*, 2011, **27**, 5665–5670.
13 A. A. Kornyshev, *et al.* Ultra-Low-Voltage Electrowetting, *J. Phys. Chem. C*, 2010, **114**, 14885–14890.
14 M. D. Dickey, *et al.* Eutectic Gallium-Indium (EGaIn): A Liquid Metal Alloy for the Formation of Stable Structures in Microchannels at Room Temperature, *Adv. Funct. Mater.*, 2008, **18**, 1097–1104.
15 M. J. Regan, *et al.* X-ray study of the oxidation of liquid-gallium surfaces, *Phys. Rev. B: Condens. Matter*, 1997, **55**, 10786–10790.
16 Y. Lin, *et al.* Handwritten, Soft Circuit Boards and Antennas Using Liquid Metal Nanoparticles, *Small*, 2015, **11**, 6397–6403.
17 I. F. Guha, J. Kedzierski and B. Abedian, Low-voltage electrowetting on a lipid bilayer formed on hafnium oxide, *Appl. Phys. Lett.*, 2011, **99**, 24105.
18 J. T. Kedzierski, R. Batra, S. Berry, I. Guha and B. Abedian, Validation of the trapped charge model of electrowetting contact angle saturation on lipid bilayers, *J. Appl. Phys.*, 2013, **114**, 24901.
19 D. J. Lomax, *et al.* Ultra-low voltage electrowetting using graphite surfaces, *Soft Matter*, 2016, **12**, 8798–8804.
20 E. Seyrat and R. A. Hayes, Amorphous fluoropolymers as insulators for reversible low-voltage electrowetting, *J. Appl. Phys.*, 2001, **90**, 1383–1386.
21 H. J. J. Verheijen and M. W. J. Prins, Reversible Electrowetting and Trapping of Charge: Model and Experiments, *Langmuir*, 1999, **15**, 6616–6620.
22 J.-H. So and M. D. Dickey, Inherently aligned microfluidic electrodes composed of liquid metal, *Lab Chip*, 2011, **11**, 905–911.
23 D. P. Parekh, C. Ladd, L. Panich, K. Moussa and M. D. Dickey, 3D printing of liquid metals as fugitive inks for fabrication of 3D microfluidic channels, *Lab Chip*, 2016, **16**, 1812–1820.
24 M. Vallet, M. Vallade and B. Berge, Limiting phenomena for the spreading of water on polymer films by electrowetting, *Eur. Phys. J. B*, 1999, **11**, 583–591.
25 A. I. Drygiannakis, A. G. Papathanasiou and A. G. Boudouvis, On the Connection between Dielectric Breakdown Strength, Trapping of Charge, and Contact Angle Saturation in Electrowetting, *Langmuir*, 2009, **25**, 147–152.
26 S. Chevalliot, S. Kuiper and J. Heikenfeld, Experimental Validation of the Invariance of Electrowetting Contact Angle Saturation, *J. Adhes. Sci. Technol.*, 2012, **26**, 1909–1930.
27 F. Mugele, Fundamental challenges in electrowetting: from equilibrium shapes to contact angle saturation and drop dynamics, *Soft Matter*, 2009, **5**, 3377.
28 A. Quinn, R. Sedev and J. Ralston, Contact Angle Saturation in Electrowetting, *J. Phys. Chem. B*, 2005, **109**, 6268–6275.
29 M. Paneru, C. Priest, R. Sedev and J. Ralston, Static and Dynamic Electrowetting of an Ionic Liquid in a Solid/Liquid/Liquid System, *J. Am. Chem. Soc.*, 2010, **132**, 8301–8308.
30 F. Li and F. Mugele, How to make sticky surfaces slippery: Contact angle hysteresis in electrowetting with alternating voltage, *Appl. Phys. Lett.*, 2008, **92**, 244108.
31 X. Tan, Z. Zhou and M. M.-C. Cheng, Electrowetting on dielectric experiments using graphene, *Nanotechnology*, 2012, **23**, 375501.
32 J. Kedzierski and S. Berry, Engineering the Electrocapillary Behavior of Electrolyte Droplets on Thin Fluoropolymer Films, *Langmuir*, 2006, **22**, 5690–5696.

Reprinted from Lab on a Chip